Full Articles

Molecular modeling of hydration properties of hydrophobic ions $Li^+@C_{60}$ and $K^+@C_{60}$

*T. Yu. Dolinina, N. S. Rusova, and V. B. Luzhkov**

Institute of Problems of Chemical Physics, Russian Academy of Sciences, 1 prosp. Akad. Semenova, 142432 Chernogolovka, Moscow Region, Russian Federation. Fax: +7 (496) 522 5636. E-mail: vbl@icp.ac.ru

The Gibbs free energies of solvation (ΔG_s) and the electronic structures of endohedral metallofullerenes $M^+@C_{60}$ ($M^+ = Li^+, K^+$) were calculated within the framework of the density functional theory and the polarizable continuum model. In water environment, the equilibrium position of K^+ is at the center of the fullerene cavity whereas that of Li^+ is shifted by 0.14 nm toward the fullerene cage. The Li^+ cation is stabilized by interactions with both the fullerene and solvent. The equilibrium structures of both endohedral metallofullerenes are characterized by very close ΔG_s values. In particular, the calculated ΔG_s values for $K^+@C_{60}$ are in the range from −124 to −149 kJ mol^{-1} depending on the basis set and on the type of the density functional. Molecular dynamics simulations (TIP3P H_2O, OPLS force field, water sphere of radius 1.9 nm) showed that the radial distribution functions of water density around C_{60} and $M^+@C_{60}$ are very similar, whereas orientations of water dipoles around the endohedral metallofullerenes resemble the hydration pattern of isolated metal ions.

Key words: fullerene, endohedral metallofullerene, the Gibbs free energy of solvation, density functional theory, polarizable continuum model, molecular dynamics, the Langevin dipoles.

Fullerene derivatives are a new interesting class of synthetic biologically active compounds (BACs). Relatively large size, regular spherical shape, and great potential of chemical modification make fullerenes, in particular, C_{60}, promising pharmacophore constituents of BACs.[1—5] Specific features of the molecular structure of fullerenes suggest that proteins and other natural biomolecules may contain fullerene-specific binding sites. In this connection, quantitative description of the effect of the fullerene fragment on the physicochemical properties of fullerene-containing compounds becomes of great importance. This first of all concerns studies of the interactions between fullerenes and their environment in biological media. Fullerenes are poorly soluble in polar solvents, show a somewhat better solubility in nonpolar aliphatic hydrocarbons, being well soluble only in aromatic hydrocarbons.[6—9] They are highly hydrophobic, readily stick to one another, and have an extremely low (not determined ex-

Published in Russian in *Izvestiya Akademii Nauk. Seriya Khimicheskaya,* No. 3, pp. 392—397, March, 2011.

1066-5285/11/6003-400

perimentally) solubility in water.[7] Nevertheless, fullerene derivatives containing polar groups can be dissolved in water with ease.[4,5]

A possible method for increasing the solubility of fullerene-containing compounds in aqueous media is the introduction of metal ions into the fullerene cage. Charged endohedral metallofullerenes can be treated as bulk hydrophobic ions. In some cases, the functional group of a charged endohedral metallofullerene can have different, as compared to the electrically neutral fullerene, binding sites to biomolecules.

The structure and dynamics of the hydration shells surrounding hydrophobic fullerene nanomolecules are also of interest from the standpoint of basic research. Until recently, ionic forms of endohedral metallofullerenes were unknown and could be treated only as hypothetical structures. However, a recently reported[10] synthesis and structural characterization of endohedral metallofullerene $Li^+@C_{60}$ likely suggests that other compounds belonging to this class can be synthesized.

The aim of the present study was to investigate the thermodynamics and structural aspects of the interactions of two endohedral metallofullerenes $M^+@C_{60}$ ($M^+ = Li^+$, K^+) with water environment by computational chemistry methods. Monatomic lithium and potassium cations were chosen as important representatives of Group I alkali metals. Experiments showed that a relatively small lithium ion encapsulated in the fullerene C_{60} cage can move within about 0.3 nm.[10] The distance allowed for the larger potassium ion to move within the C_{60} sphere seems to be shorter. In the present work, we calculated the Gibbs free energies of solvation (ΔG_s) of the title hydrophobic ions in water. By definition, ΔG_s is the Gibbs free energy of transfer of a compound from the gas phase to a solution (see, *e.g.*, Ref. 11). To date, the experimental ΔG_s values for water have not been determined for all known fullerenes. In the present work, the ΔG_s values were estimated within the framework of the density functional theory (DFT) and the polarizable continuum model (PCM). Also, the molecular dynamics (MD) simulations for microscopic models for the hydrated metallofullerenes $M^+@C_{60}$ were carried out. Some problems in research on the physicochemical properties of fullerenes in solution were investigated earlier by both DFT [12—14] and MD methods.[15—20]

Calculation Procedure

The Gibbs free energies of solvation of $M^+@C_{60}$ were calculated within the framework of the DFT and the PCM model using the Gaussian-03 program.[21] The solvation model used is based on representation of the solvent by a continuous polarizable medium in which the solute molecule forms a cavity with a well-defined boundary. The standard Gibbs free energy of solvation ΔG_s is calculated in the PCM as the sum of the following contributions

$$\Delta G_s = \Delta G_{el} + \Delta G_{cav} + \Delta G_{disp} + \Delta G_{rep},$$

where ΔG_{el} is the energy of electrostatic interaction of solute molecules with the dielectric continuum (including their mutual polarization), ΔG_{cav} is the Gibbs free energy of formation of a cavity in the dielectric medium, ΔG_{disp} is the energy of dispersion interaction, and ΔG_{rep} is the electron-electron repulsion energy.[22—24] The universal force field[21] (UFF) parameterization of atomic radii was used. In constructing the solvent cavity the molecular surfaces were augmented with (*i*) a sphere of radius 0.324 nm inscribed into the C_{60} cage and centered at the center of the fullerene molecule and (*ii*) spherical fragments to smooth the outer surface of the molecule (the last-mentioned procedure is by default used in the Gaussian-03 program).[21] The fullerene wave functions were calculated in the 6-31G(d), 6-31+G(d), and LANL2DZ basis sets[21,25] (LANL2DZ is the basis set optimized for the alkali metal calculations). The results obtained with a number of DFT computational schemes using various exchange and correlation functionals were analyzed. Three-dimensional structures of endohedral metallofullerenes were constructed based on the experimental data for C_{60} thiophene disolvate[26] (localization of the alkali metal ion was studied additionally).

MD calculations were performed for the fullerenes located at the center of a water sphere of radius 1.9 nm comprising 922 water molecules. Potential energy calculations were carried out using the OPLS force field;[27] the potentials of nonbonding site—site interactions were specified as follows:

$$U(r_{ij}) = 4\varepsilon_{ij}[(\sigma_{ij}/r_{ij})^{12} - (\sigma_{ij}/r_{ij})^6] + q_i q_j / r_{ij},$$

where *i* and *j* enumerate atoms belonging to different molecules, and included contributions from the dispersion and Coulomb interactions and the electron—electron repulsion energies. In particular, the Lennard-Jones parameters of aromatic carbon atoms ($\sigma_i = 0.355$ nm, $\varepsilon_i = 0.070$ kJ mol^{-1}) were used for C_{60}. The atomic charges q_i were estimated from DFT calculations; for $K^+@C_{60}$, they are 0.880 on K and 0.002 on C. The 6—5 and 6—6 bond lengths in the C_{60} molecule were set equal to 0.1385 and 0.1451 nm, respectively, taking into account the X-ray data.[26] The TIP3P parameters ($\sigma_i(O) = 0.315$ nm, $\varepsilon_i(O) = 0.636$ kJ mol^{-1}, $q_i(O) = -0.834$)[28] were used for water molecules; the cations parameters taken from Ref. 29 were as follows: $\sigma_i = 0.213$ nm, $\varepsilon_i = 0.076$ kJ mol^{-1} for Li^+ and $\sigma_i = 0.494$ nm, $\varepsilon_i = 0.001$ kJ mol^{-1} for K^+. Molecular simulation was carried out using a localized parallel version of an MD program.[30] The SCAAS spherical boundary conditions[31] were taken into account for the water drop. Water molecules and fullerene were considered rigid within the SHAKE algorithm.[32] The fullerene carbon atoms were restrained with a harmonic potential to hold them together within a sphere of radius 0.37 nm (if the distance from a given C atom to the center of the system was shorter than 0.37 nm, the restraining potential was set equal to zero; at distances longer than 0.37 nm, the atom was in a harmonic potential with a constant of 20.9 kJ mol^{-1}). MD calculations were performed for $T = 300$ K using a thermostat relaxation time $\tau_T = 0.2$ ps and a time step of 2 fs. In calculations of the radial distribution functions (RDF) the model systems were equilibrated over a period of 5 ns, followed by a 2 ns MD simulation after each five

steps on the MD trajectory. The RDF for the orientation of water dipoles

$$f_\theta(r) \equiv \langle \cos(\theta) \rangle = \langle (\vec{\mu}_w / \vec{r}_w) \rangle / (\mu_w / r_w)$$

were calculated taking into account the histograms of the cosine of the orientation angle of the water dipole vector $\vec{\mu}_w$ in the corresponding spherical layer of the solvent. The radius-vector $\vec{r}_w$ of the center of a point water dipole was calculated by a rigorous expression

$$\vec{r}_w = \vec{r}_O/2 + \vec{r}_{H(1)}/4 + \vec{r}_{H(2)}/4.$$

The radius of the spherical cells for constructing the RDF histograms was 0.005 nm.

Results and Discussion

In studies of the structures of charged endohedral metallofullerenes, an important issue is location of the metal ion within the fullerene cage. The results of B3LYP/LANL2DZ calculations of the energy characteristics of the motion of the Li^+ and K^+ ions from the center of the fullerene sphere toward the center of a hexagon carried out with inclusion of the solvent effect are shown in Fig. 1. The ion motion coordinate was chosen based on experimental data.[10] According to calculations, transition of $M^+@C_{60}$ from the gas phase to the aqueous medium is exothermic (see also Table 1). From the plots in Fig. 1 it also follows that the total energy (E_{tot}) minimum for $Li^+@C_{60}$ in the gas phase is attained at a distance $\Delta r_{min} \approx$ ≈ 0.14 nm from the center. Displacement of Li^+ to the outermost position relative to the center causes $\Delta G_s(Li^+@C_{60})$ to decrease by about 5 kJ mol^{-1}. Thus, Li^+ displaced from the center toward the inner surface of C_{60} fullerene is stabilized by both intramolecular interactions and interactions with water. For $K^+@C_{60}$, the minimum of E_{tot} corresponds to $\Delta r_{min} = 0$. In the range of allowed Δr values, changes in ΔG_s for K^+ are small, being at most 0.1 kJ mol^{-1}. Consideration of the total energies in solution causes no changes in position of the total energy minimum compared to the gas-phase case. The equilibrium Δr_{min} values for both endohedral metallofullerenes also remain unchanged when using the B3PW91 instead of B3LYP functional. The results of calculations are in good agreement with the experimental position of the Li^+ ion ($\Delta r_{min} =$ $= 0.134$ nm) in the $Li^+@C_{60}$ complex with the $SbCl_6^-$ counterion.[10] By and large, the positions of the minima in Fig. 1 are in qualitative agreement with the radii of the ions in question. For instance, the van der Waals parameters σ_{ij} of the interactions between K^+ and C atoms are 0.068 nm larger than the average distance $\langle r(\text{center—C}) \rangle =$ $= 0.351$ nm from the C atoms to the center of the C_{60} sphere; this suggests localization of the ions at the center of the fullerene cage. Contrary to this, the σ_{ij} parameters for Li^+ and C atoms is 0.076 nm smaller than $\langle r(\text{center—C}) \rangle$.

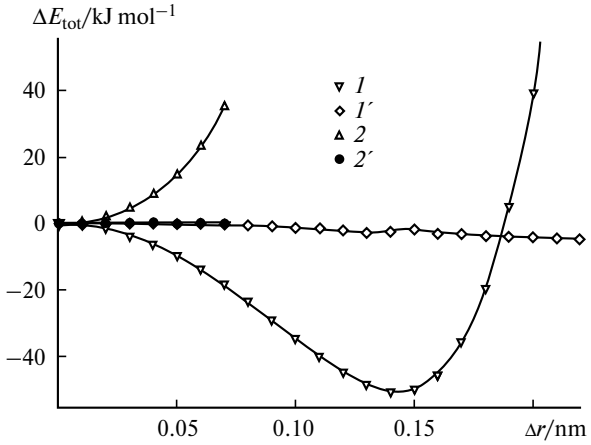

Fig. 1. Total energies (ΔE_{tot}) plotted *vs.* displacement (Δr) of the ion from the center of the fullerene cage along a straight line to the center of a hexagon: changes in the total energies of isolated $Li^+@C_{60}$ (*1*) and $K^+@C_{60}$ (*2*), electrostatic contribution to the relative energies of hydration $Li^+@C_{60}$ (*1′*) and $K^+@C_{60}$ (*2′*). Obtained from B3LYP/LANL2DZ/PCM calculations.

The results of calculations of the Gibbs free energies of solvation $\Delta G_s(M^+@C_{60})$ are listed in Tables 1 and 2. The data in Table 1 characterize how the changes in the basis set and in the shape of the potential affect the energy characteristics of $K^+@C_{60}$ with rigid geometry. The $\Delta G_s(K^+@C_{60})$ values lie between -124 and -149 kJ mol^{-1}. A comparison of the results obtained using three basis sets (see Table 1) shows that the smallest negative ΔG_s values were obtained in calculations with the 6-31G(d) basis set. Augmentation with diffuse functions on going from the 6-31G(d) to the 6-31+G(d) basis set causes ΔG_s to become more negative (by 5—10 kJ mol^{-1}). The ΔG_s values obtained from calculations with the LANL2DZ basis set are even more negative (by 1—10 kJ mol^{-1}). The ΔG_s values obtained using different density functionals and the same basis set differ insignificantly, whereas the Hartree—Fock calculations give the largest negative values in all cases. Note that calculations by all methods predict positive ΔG_s values for the fullerene C_{60}, *e.g.*, $\Delta G_s(C_{60}) = 14.8$ kJ mol^{-1} according to B3PW91/LANL2DZ calculations.

The contributions to ΔG_s calculated for the endohedral metallofullerenes by the B3LYP/LANL2DZ method using the equilibrium Δr_{min} values are listed in Table 2. The net nonpolar contributions for $Li^+@C_{60}$ and $K^+@C_{60}$ are +24.2 and +22.4 kJ mol^{-1}, respectively, thus being small compared to the energy of electrostatic interactions. The total value of $\Delta G_s(Li^+@C_{60})$ is -137.9 kJ mol^{-1}, which is very close to $\Delta G_s(K^+@C_{60}) = -137.5$ kJ mol^{-1}. The ΔG_{el} and ΔG_s values calculated by the B3LYP/LANL2DZ method for the ions located at the center of the cage ($\Delta r = 0$) are respectively -159.7 and -159.9 kJ mol^{-1} for $Li^+@C_{60}$ and -135.4 and -137.5 kJ mol^{-1} for $K^+@C_{60}$. The difference $\Delta G_s = 2.1$ kJ mol^{-1} is mainly due to the contribution of

Table 1. The Gibbs free energies of solvation (ΔG_s/kJ mol^{-1}) and the electron charges (q/e) of $K^+@C_{60}$[a] calculated by different methods using the 6-31G(d), G-31+(d), and LANL2DZ basis sets

Computational method	6-31G(d)			6-31+G(d)			LANL2DZ		
	$-\Delta G_s$[b]	q_K(Mull)[c]	q_K(NAO)[c]	$-\Delta G_s$	q_K(Mull)	q_K(NAO)	$-\Delta G_s$	q_K(Mull)	q_K(NAO)
HF[d]	131.2	0.99	0.92	139.6	1.15	0.87	149.2	1.02	0.88
SWVN[e]	123.7	0.79	0.90	130.7	0.49	0.87	134.2	0.81	0.90
OPBE[e]	124.1	1.16	0.91	128.9	1.56	0.86	133.2	1.14	0.89
OLYP[e]	124.7	1.02	0.92	132.8	1.29	0.86	134.6	1.00	0.89
BLYP[e]	125.2	0.76	0.91	135.0	0.48	0.87	135.8	0.76	0.90
B3LYP[e]	125.9	0.83	0.91	134.5	0.61	0.87	137.5	0.83	0.90
B3PW91[e]	125.4	0.93	0.91	131.3	0.77	0.87	136.2	0.92	0.89

[a] Calculations for $\Delta r_{min}(K^+)$.
[b] The sum of nonpolar contributions to ΔG_s is 22.4 kJ mol^{-1}.
[c] q_K(Mull) and q_K(NAO) are the electron density on K^+ calculated according to Mulliken and for the natural orbitals, respectively.
[d] Hartree—Fock calculations.
[e] Density functional.[20]

dispersion interaction. As mentioned above, displacement of the Li^+ ion from the center of the cage toward the equilibrium position causes $\Delta G_s(Li^+@C_{60})$ to be close to $\Delta G_s(K^+@C_{60})$. Thus, the data in Tables 1 and 2 show that, in spite of different positions of the alkali metal ions within the fullerene cage, $Li^+@C_{60}$ and $K^+@C_{60}$ are stabilized in a similar manner in water environment. This is in high contrast with the difference between the experimental ΔG_s values for these ions in water, *viz.*, −476 and −511 kJ mol^{-1} (see Refs 33 and 29, respectively) for Li^+ and −298 and −337 kJ mol^{-1} (see Refs 33 and 29, respectively) for K^+. The experimental values of the Gibbs free energies of solvation of $M^+@C_{60}$ are unknown; however, the calculated ΔG_s values agree with the published data on hydration of bulky hydrophobic ions, *e.g.*, PPh_4^+ and $AsPh_4^+$,[34] as well as $(n\text{-}C_3H_7)_4N^+$ and $(n\text{-}C_5H_{11})_4N^+$.[35]

Table 1 also lists the data characterizing the electron density distribution in $K^+@C_{60}$. The Mulliken atomic charges of K^+, q_K(Mull), are scattered between 0.48 and 1.56. The largest variations of q_K(Mull) were obtained with the 6-31+G(d) basis set augmented with diffuse orbitals. At the same time, calculations of the electron density for the natural orbitals q_K(NAO)[36] in all cases predict a K^+ charge of about 0.9, which corresponds to transfer of nearly 0.1e from the fullerene cage to the central metal ion.

Table 2. Contributions to the Gibbs free energies of solvation $\Delta G_s(M^+@C_{60})$ for the equilibrium positions of ions obtained from B3LYP/LANL2DZ/PCM calculations

Compound	Δr_{min} /nm	ΔG_{cav}	$-\Delta G_{disp}$	ΔG_{rep}	$-\Delta G_{s,el}$	$-\Delta G_s$
		kJ mol^{-1}				
$Li^+@C_{60}$	0.14	187.3	172.8	9.7	162.2	137.9
$K^+@C_{60}$	0	187.3	174.6	9.7	159.9	137.5

The much weaker dependence of q(NAO), compared to q(Mull), on the computational method was reported for many systems.[37] For $K^+@C_{60}$, the best agreement between q(Mull) and q(NAO) was obtained from the B3PW91/LANL2DZ calculations (see Table 1). B3LYP/LANL2DZ calculations of the electron density in $Li^+@C_{60}$ for the equilibrium Δr_{min} value gave q_K(Mull) = 0.62 and q_K(NAO) = 0.89; no marked nonuniformity of the electron density distribution over the fullerene carbon atoms was revealed. By and large, the atomic charges in $Li^+@C_{60}$ and $K^+@C_{60}$ appeared to be close. The q(NAO) charges were used in subsequent MD simulations using microscopic models for endohedral metallofullerenes.

A limitation of the macroscopic description of hydration effects is the lack of information on the spatial distribution and polarization of water molecules surrounding the solute. To evaluate these effects, in the present work we studied the molecular dynamics of K^+, C_{60}, $Li^+@C_{60}$, and $K^+@C_{60}$ for the microscopic model of a water sphere (Fig. 2) and calculated the corresponding RDF of water molecules.

The $g_O(r)$ plots for the density of water O atoms (Fig. 3) show differences between the RDF for $Li^+@C_{60}$ and $K^+@C_{60}$. In the former case, the calculated distribution exhibits a flat shoulder toward the central ion, which is due to the displacement of Li^+ toward the inner surface of fullerene. However, maxima in both plots (see Fig. 3) are at nearly the same positions. A comparison of the $g_O(r)$ and $g_H(r)$ plots for the density of water (see Figs 3 and 4) shows that the RDF around the central ion of $M^+@C_{60}$ are similar to the RDF of fullerene C_{60}. Transition from the idealized charge distribution to the q(NAO) charges (*cf.* Figs 3 and 4) has little effect and manifests itself in the case of q(NAO) as a somewhat longer shoulder in the RDF for the density of water and a somewhat more "fixed" orientation of water dipoles at short distances. The RDF calculated for C_{60} are in good agreement with the pub-

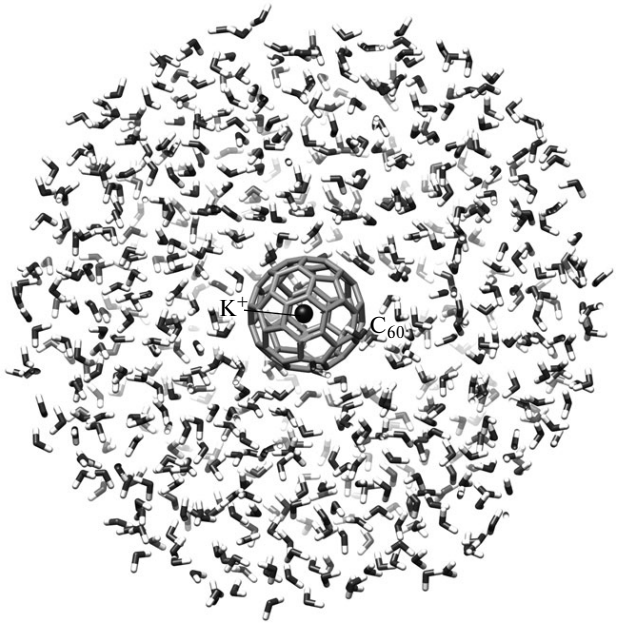

Fig. 2. Model for MD calculations: an endohedral metallofullerene surrounded by H_2O molecules from a water sphere of radius 1.9 nm.

lished data[19] obtained for the "simple point charge" model of H_2O and periodic boundary conditions. In regard to the effects of the charge of the metallofullerene, it should be noted that the $g_O(r)$ RDF of the K^+ ion in solution (see Fig. 4) is close to unity at the distances corresponding to the first maximum of $g_O(r)$ for C_{60} and, therefore, the effect of the central ion in $K^+@C_{60}$ on the density of water at the corresponding distances is rather weak. Nevertheless, the distributions $f_\theta(r)$ of the average cosine of the orientation angle of the water dipole vector $\vec{\mu}_w$ for C_{60} and $K^+@C_{60}$ are different (Fig. 5). The $\langle\cos(\theta)\rangle$ values for C_{60} are quite small at all distances from the center except a small peak in the zone of direct contact between water molecules and fullerene surface. For $K^+@C_{60}$, the $f_\theta(r)$ peak in positions of direct contact with water is much higher than for C_{60} due to the effect of the electric charge of the endohedral metallofullerene. The $f_\theta(r)$ plots show that the orientational ordering of water molecules at the contact distances around $K^+@C_{60}$ is higher than around K^+ at the same distances. Thus, the fullerene cage also to some extent affects the orientations of water molecules in the first hydration shell.

It is interesting to compare the analytical estimate of $\langle\cos(\theta)\rangle$ obtained using the Langevin formula (see, *e.g.*, Refs 34 and 38) with the $g_O(r)$ values obtained from MD calculations. The Langevin formula gives an average cosine of the angle between a point dipole vector $\vec{\mu}$ and the

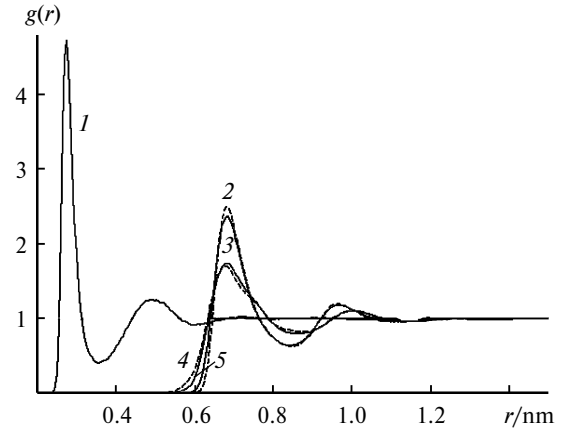

Fig. 4. The RDF of the density of O (*1*—*3*) and H (*4*, *5*) atoms of water for K^+ (*1*), C_{60} (*2*, *4*) and $K^+@C_{60}$ (*3*, *5*). Atomic charges in the endometallofullerene were chosen based on the *q*(NAO) values obtained from DFT calculations.

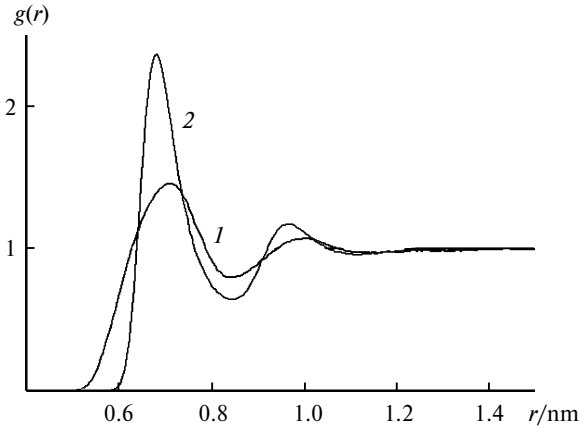

Fig. 3. The RDF of the density of water O atoms for $Li^+@C_{60}$ (*1*) and $K^+@C_{60}$ (*2*) plotted based on the MD trajectories depending on the distance to the central atom *r*. The charge on the central ion was set to +1.

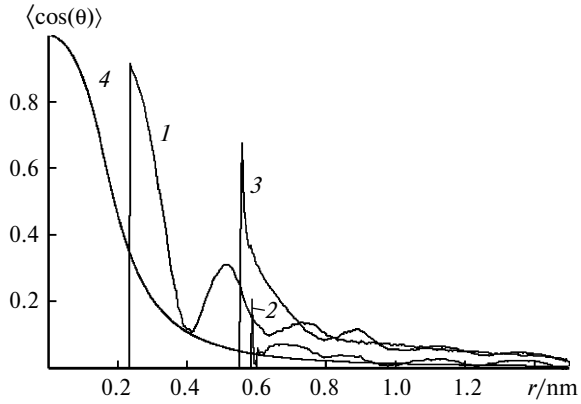

Fig. 5. Average orientation of water dipoles $\langle\cos(\theta)\rangle$ for K^+ (*1*), C_{60} (*2*) and $K^+@C_{60}$ (*3*) as a function of the distance to the central atom *r*. Atomic charges of the endohedral metallofullerene were chosen in accordance with the *q*(NAO) values, the Langevin function (*4*) was calculated taking into account the distance-dependent water dipole shielding function.

effective electric field $\vec{E}$ under thermal equilibrium conditions:

$$\langle\cos(\theta)\rangle = L(\beta\mu E) = \frac{\exp(\beta\mu E) + \exp(-\beta\mu E)}{\exp(\beta\mu E) - \exp(-\beta\mu E)} - \frac{1}{\beta\mu E}, \quad (1)$$

where $\beta = 1/(kT)$, k is the Boltzmann constant, and T is absolute temperature (K). The energy of a point dipole $\vec{\mu}$ in the field created by a point charge q depends on the distance r between them:

$$W(r) = -2.89q\vec{\mu}\vec{r}/r^3, \quad (2)$$

where W is expressed in kJ mol^{-1}, μ is expressed in D, and r is expressed in nm. For $q = +1$, μ_w(TIP3P) = 2.35 D, and taking into account the distance-dependent shielding function of the electric field of the solvent $\varepsilon_w(r)$,[38] substitution of expression (2) to Eq. (1) gives an analytical dependence of $\langle\cos(\theta)\rangle$ on r (see the plot in Fig. 5). In this case, the Langevin formula predicts a somewhat faster decrease in $\langle\cos(\theta)\rangle$ at short r compared to the results of MD calculations. The difference can be due to the fact that the parameteric relation for $\varepsilon_w(r)$ was derived based on the calculations of the enthalpies of hydration within the framework of a continuum description of the solvent,[38] whereas the effective value of $\varepsilon_w(r)$ at short distances can be somewhat smaller for the model in which water molecules are specified explicitly. It should be noted that the $f_\theta(r)$ curves calculated by molecular simulation have a wave-like shape in contrast to the smooth curve of the Langevin function.

Thus, our study showed that hydrophobic ions of endohedral metallofullerenes with encapsulated alkali metal cations are characterized by negative hydration energy, which may provide a rather high solubility of these systems in water. At the same time, ΔG_s are low in absolute value; this reduces the permeability barrier through nonpolar biomembranes. The endohedral metallofullerenes $Li^+@C_{60}$ and $K^+@C_{60}$ are characterized by close ΔG_s values in spite of different equilibrium positions of the central ions. The fullerene carbon cage has a crucial effect on the RDF of the density of water molecules surrounding the charged endohedral metallofullerene. The influence of the positive charge of $M^+@C_{60}$ is reduced to pronounced orientational effect on the H_2O molecules. Such properties of charged endohedral metallofullerenes can be important in the design of BACs based on them. Investigations of fullerene binding to biomolecules are planned for the future.

The authors express their gratitude to A. S. Zyubin for useful discussions and to the Computing Center of the Institute of Problems of Chemical Physics, Russian Academy of Sciences, and the Landau Institute of Theoretical Physics, Russian Academy of Sciences, for help in performing calculations.

This work was financially supported by the Presidium of the Russian Academy of Sciences (Basic Research Program No. 22, Research Avenue 2.3).

References

1. S. H. Friedman, P. S. Ganapathi, Y. Rubin, G. L. Kenyon, *J. Med. Chem.*, 1998, **41**, 2424.
2. S. R. Wilson, in *Fullerenes. Chemistry, Physics, and Technology*, Eds K. K. Kadish, R. S. Ruoff, Wiley-Interscience, New York, 2000, p. 437.
3. S. Bosi, T. Da Ros, G. Spalluto, J. Balzarini, M. Prato, *Bioorg. Med. Chem. Lett.*, 2003, **13**, 4437.
4. E. Nakamura, H. Isobe, in *Dekker Encyclopedia of Nanoscience and Nanotechnology*, 2nd ed., Eds C. I. Contescu, K. Putyera, CRC Press, New York, 2009, Ch. 285, 3277.
5. P. A. Troshin, O. A. Troshina, R. N. Lyubovskaya, V. F. Razumov, *Funktsional´nye proizvodnye fullerenov: metody sinteza i perspektivy ispol´zovaniya v organicheskoi elektronike i biomeditsine [Functional Derivatives of Fullerenes: Methods of Synthesis and Prospects for Organic Electronics and Biomedical Applications]*, Izd. IvGU, Ivanovo, 2nd Ed., 2010, 340 pp. (in Russian).
6. R. S. Ruoff, D. S. Tse, R. Malhotra, D. C. Lorents, *J. Phys. Chem.*, 1993, **97**, 3379.
7. D. Heyman, *Fullerene Sci. Technol.*, 1996, **4**, 509.
8. M. V. Korobov, A. L. Smith, in *Fullerenes. Chemistry, Physics, and Technology*, Eds K. K. Kadish, R. S. Ruoff, Wiley-Interscience, New York, 2000, p. 53.
9. P. P. Kulkarni, C. T. Jafvert, *Environ. Sci. Technol.*, 2008, **42**, 845.
10. S. Aoyagi, E. Nishibori, H. Sawa, K. Sugimoto, M. Takata, Y. Miyata, R. Kitaura, H. Shinohara, H. Okada, T. Sakai, Y. Ono, K. Kawachi, K. Yokoo, S. Ono, K. Omote, Y. Kasama, S. Ishikawa, T. Komuro, H. Tobita, *Nature Chem.*, 2010, **2**, 678.
11. N. M. Bazhin, V. A. Ivanchenko, V. N. Parmon, *Termodinamika dlya khimikov [Thermodynamics for Chemists]*, Khimiya, Moscow, 2nd Ed., 2004, 416 pp. (in Russian).
12. W. Andreoni, A. Curioni, *Appl. Phys. A*, 1997, **66**, 299.
13. W. Andreoni, *Ann. Rev. Phys. Chem.*, 1998, **49**, 405.
14. E. B. Stukalin, M. V. Korobov, N. V. Avramenko, *J. Phys. Chem. B*, 2003, **107**, 9692.
15. T. Werder, J. H. Walther, R. L. Jaffe, T. Halicioglu, P. Koumoutsakos, *J. Phys. Chem. B*, 2003, **107**, 1345.
16. T. Hotta, A. Kimura, M. Sasai, *J. Phys. Chem. B*, 2005, **109**, 18600.
17. R. Chang, A. Violi, *J. Phys. Chem. B*, 2006, **110**, 5073.
18. L. Li, D. Bedrov, G. D. Smith, *J. Phys. Chem. B*, 2006, **110**, 10509.
19. D. R. Weiss, T. M. Raschke, M. Levitt, *J. Phys. Chem. B*, 2008, **112**, 2981.
20. C. Maciel, E. E. Fileti, R. Rivelino, *J. Phys. Chem. B*, 2009, **113**, 7045.
21. M. J. Frisch, G. W. Trucks, H. B. Schlegel, G. E. Scuseria, M. A. Robb, J. R. Cheeseman, J. A. Montgomery, Jr., T. Vreven, K. N. Kudin, J. C. Burant, J. M. Millam, S. S. Iyengar, J. Tomasi, V. Barone, B. Mennucci, M. Cossi, G. Scalmani, N. Rega, G. A. Petersson, H. Nakatsuji, M. Hada, M. Ehara, K. Toyota, R. Fukuda, J. Hasegawa,

M. Ishida, T. Nakajima, Y. Honda, O. Kitao, H. Nakai, M. Klene, X. Li, J. E. Knox, H. P. Hratchian, J. B. Cross, V. Bakken, C. Adamo, J. Jaramillo, R. Gomperts, R. E. Stratmann, O. Yazyev, A. J. Austin, R. Cammi, C. Pomelli, J. W. Ochterski, P. Y. Ayala, K. Morokuma, G. A. Voth, P. Salvador, J. J. Dannenberg, V. G. Zakrzewski, S. Dapprich, A. D. Daniels, M. C. Strain, O. Farkas, D. K. Malick, A. D. Rabuck, K. Raghavachari, J. B. Foresman, J. V. Ortiz, Q. Cui, A. G. Baboul, S. Clifford, J. Cioslowski, B. B. Stefanov, G. Liu, A. Liashenko, P. Piskorz, I. Komaromi, R. L. Martin, D. J. Fox, T. Keith, M. A. Al-Laham, C. Y. Peng, A. Nanayakkara, M. Challacombe, P. M. W. Gill, B. Johnson, W. Chen, M. W. Wong, C. Gonzalez, J. A. Pople, *Gaussian 03*, *Revision D. 01*, Gaussian, Inc., Wallingford (CT), 2004.

22. B. Mennucci, E. Cancès, J. Tomasi, *J. Phys. Chem. B*, 1997, **101**, 10506.
23. V. Barone, M. Cossi, J. Tomasi, *J. Chem. Phys.*, 1997, **107**, 3210.
24. M. Cossi, G. Scalmani, N. Rega, V. Barone, *J. Chem. Phys.*, 2002, **117**, 43,
25. P. J. Hay, W. R. Wadt, *J. Chem. Phys.*, 1985, **82**, 299.
26. A. D. Bond, *Acta Crystallogr. E*, 2003, **E59**, o1992.
27. W. L. Jorgensen, D. S. Maxwell, J. Tirado-Rives, *J. Am. Chem. Soc.*, 1996, **118**, 11225.
28. W. L. Jorgensen, J. Chandrasekhar, J. D. Madura, R. W. Imprey, M. L. Klein, *J. Chem. Phys.*, 1983, **79**, 926.
29. J. Åqvist, *J. Phys. Chem.*, 1990, **94**, 8021.
30. J. Marelius, K. Kolmodin, I. Feieberg, J. Åqvist, *J. Mol. Graphics Modell.*, 1999, **16**, 213.
31. G. King, A. Warshel, *J. Chem. Phys.*, 1989, **91**, 3647.
32. J.-P. Ryckaert, G. Cicotti, H. J. C. Berendsen, *J. Comput. Phys.*, 1977, **23**, 327.
33. R. Schmid, A. M. Miah, V. N. Sapunov, *Phys. Chem. Chem. Phys.*, 2000, **2**, 97.
34. V. Luzhkov, A. Warshel, *J. Comput. Chem.*, 1992, **13**, 199.
35. V. B Luzhkov, F. Österberg, P. Acharya, J. Chattopadhyaya, J. Åqvist, *Phys. Chem. Chem. Phys.*, 2002, **4**, 4640.
36. A. E. Reed, L. A. Curtiss, F. Weinhold, *Chem. Rev.*, 1988, **88**, 899.
37. F. Jensen, *Introduction to Computational Chemistry*, Wiley, Chichester, 1999, 429 p.
38. V. B. Luzhkov, *Izv. Akad. Nauk, Ser. Khim.*, 1999, 1232 [*Russ. Chem. Bull.* (*Engl. Transl.*), 1999, **48**, 1219].

Received September 17, 2010